21. D. K. Morrison, unpublished data.
22. B. C. Turner, N. K. Tonks, U. R. Rapp, J. C. Reed, *Proc. Natl. Acad. Sci. U.S.A.* **90**, 5544 (1993).
23. F. Chen and P. D. Wagner, *FEBS Lett.* **347**, 128 (1994).
24. Y. Furukawa *et al.*, *Biochem. Biophys. Res. Commun.* **194**, 144 (1993).
25. Plasma membranes were purified as described by flotation on discontinuous sucrose gradients (*4*), resuspended (1 mg/ml) in buffer E [25 mM Hepes (pH 7.4 at 30°C), 10 mM EDTA, 10 mM EGTA] containing the specified mix of protease inhibitors (*4*), kept on ice, and used immediately. Equal portions of resuspended plasma membranes from v-*ras*–transformed NIH 3T3 cells and v-*src*–transformed Raf-1 cells (5 to 10 100-mm dishes, each) were combined and sonicated (three 20-s bursts) on ice in a bath sonicator (model G112SP1G; Laboratory Supply, Hicksville, NY). Sonicated plasma membranes (0.1 ml, 0.1 mg of total protein) were then incubated (30°C, 15 min) in the absence or presence of 1 mM GTP and protein phosphatase inhibitors (final concentrations: 10 μM microcystin-LR, 100 μM inhibitor-2, 0.2 mM sodium orthovanadate). Membranes from each condition were centrifuged (100,000*g*, 15 min, 4°C) in an Airfuge (Beckman, Palo Alto, CA) and resuspended in buffer E to a volume of 0.1 ml. No appreciable losses of total membrane or Raf-1 protein occurred. Raf-1 is not appreciably dissociated from immobilized Ras-GTP by chelators (*17*), consistent with the observation that dissociation of guanine nucleotide from Ras is negligible in the absence of competing nucleotide [A. Hall and A. J. Self, *J. Biol. Chem.* **261**, 10963 (1986)].
26. M. G. Pan, T. Florio, P. Stork, *Science* **256**, 1215 (1992).
27. M. J. Hubbard and P. Cohen, *Trends Biochem. Sci.* **18**, 172 (1993).
28. D. Barford, A. J. Flint, N. K. Tonks, *Science* **263**, 1397 (1994).
29. We thank P. Cohen and D. Brautigan for PP1; T. Haystead and D. Brautigan for PP2A; N. Tonks for PTP1B and catalytically inactive PTP1B; D. Pallas for recombinant 14-3-3ζ; K. Zeller, L. A. Vincent, and C. Harrison for technical assistance; and D. Brautigan for helpful discussions. Supported by the Howard Hughes Medical Institute and by grants from NIH to T.W.S. (DK41077) and to M.J.W. (GM47322), and from the American Cancer Society to T.W.S. (BE69D) and by contract to D.K.M. (N01-CO-46000). P.D. is a postdoctoral fellow of the Juvenile Diabetes Foundation International.

23 January 1995; accepted 26 April

Requirement for TNF-α and IL-1α in Fetal Thymocyte Commitment and Differentiation

Juan Carlos Zúñiga-Pflücker,* Di Jiang, Michael J. Lenardo

CD25 expression occurs early in thymocyte differentiation. The mechanism of induction of CD25 before T cell receptor rearrangement and the importance of this mechanism for T cell development are unknown. In a thymus reconstitution assay, tumor necrosis factor α (TNF-α) and interleukin-1α (IL-1α), two cytokines produced within the thymic microenvironment, induced CD25 expression on early immature thymocytes. Either TNF-α or IL-1α was necessary for further thymocyte maturation and $CD4^+CD8^+$ differentiation. In irradiated mice reconstituted with $CD117^+CD25^+$ thymocytes, commitment to the T cell lineage was marked by the loss of precursor multipotency.

An important question in developmental biology is the nature of the molecular signals that occur between interacting tissues during organogenesis. In the immune system, the thymus is formed when the rudimentary thymic stroma is colonized by fetal liver–derived hematopoietic stem cells at day 12 of fetal life, and it provides the necessary elements for the commitment and differentiation of stem cells into T cells (*1*, *2*). During early fetal thymic development, it is unclear when commitment to the T lineage occurs. Newly arrived thymic lymphocyte precursors express CD117 (c-kit), which is the receptor for stem cell factor (SCF) and identifies cells from the fetal liver, bone marrow, and thymus that display hematopoietic stem cell function (*3*). The loss of CD117, beginning approximately at day 15, correlates with initiation of T cell receptor (TCR) β-chain rearrangement (*3*). The next step in thymocyte maturation is associated, in both mouse and human, with the expression of CD25 (IL-2 receptor α chain) (*4*); however, it is apparent that binding of IL-2 is not required for normal thymus development (*5*). Nevertheless, $CD25^+$ thymocytes predominate at days 14 and 15 of mouse fetal development (Fig. 1A) and express gene regulatory proteins and surface proteins that are characteristic of antigen-activated mature T cells (*6*). Although mature T cells express CD25 after TCR ligation (*7*), CD25 expression by $CD117^+$ immature thymocytes occurs before TCR rearrangement. We therefore investigated the molecular mechanism of CD25 induction and its significance in thymocyte differentiation and commitment to the T lineage.

To study CD25 induction, we prepared

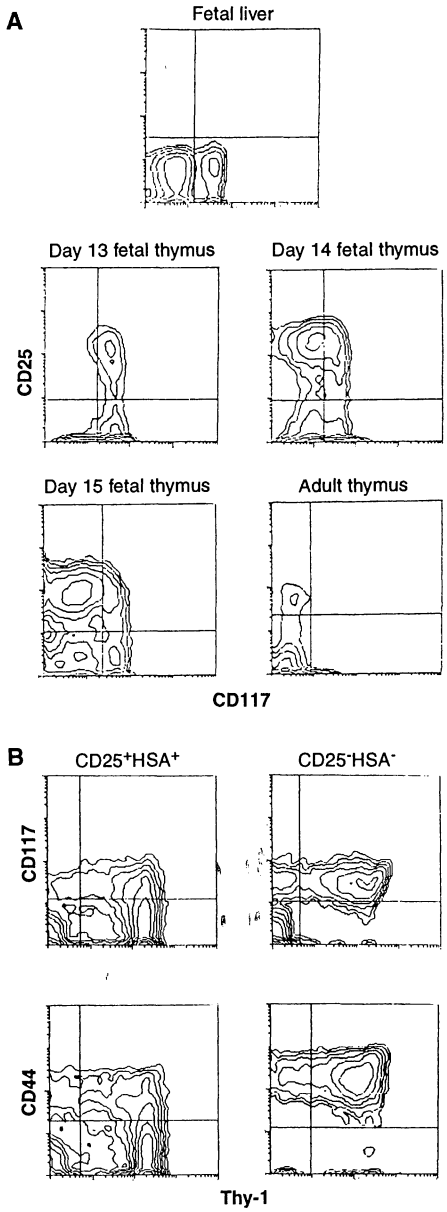

Fig. 1. T cells go through a $CD117^+CD25^+$ stage during early fetal thymic development. (**A**) CD25 and CD117 expression as a function of time in mouse fetal thymic development and in day 13 fetal liver (*15*). Percent staining for CD117 versus CD25 is given for the upper left (UL), upper right (UR), lower left (LL), and lower right (LR) areas of the flow cytometry plots. Fetal liver cells, UL, 0.0%; UR, 0.5%; LL, 78.7%; and LR, 20.7%. Day 13 fetal thymus, UL, 4.7%; UR, 27.0%; LL, 21.8%; and LR, 46.5%. Day 14 fetal thymus, UL, 35.1%; UR, 24.2%; LL, 22.6%; and LR, 18.1%. Day 15 fetal thymus, UL, 59.1%; UR, 9.4%; LL, 24.3%; and LR, 7.2%. Adult thymus, UL, 11.6%; UR, 1.8%; LL, 81.2%; and LR, 5.45%. (**B**) Phenotype of the HSA^-CD25^- SCID immature thymocytes prepared by treatment with antibody and complement elimination of later thymocyte stages (*16*). Percent staining for Thy-1 versus CD117: $CD25^+HSA^+$ thymocytes (not treated), UL, 1.9%; UR, 18.2%; LL, 14.3%; and LR, 65.5%. $CD25^-HSA^-$ thymocytes (treated), UL, 7.8%; UR, 45.6%; LL, 44.2%; and LR, 2.3%. Percent staining for Thy-1 versus CD44: $CD25^+HSA^+$ thymocytes, UL, 2.3%; UR, 18.7%; LL, 6.7%; and LR, 72.3%. $CD25^-HSA^-$ thymocytes, UL, 13.7%; UR, 83.4%; LL, 1.2%; and LR, 1.7%.

Laboratory of Immunology, National Institute of Allergy and Infectious Diseases, Bethesda, MD 20892, USA.

*Present address: University of Toronto, Department of Immunology, Medical Sciences Building, Toronto, Ontario M5S 1A8, Canada.

immature thymocytes by means of antibody- and complement-mediated depletion of more mature thymocytes that expressed CD25, heat-stable antigen (HSA), or both. Treated day 15 fetal thymocytes or thymocytes from neonatal mice with severe combined immunodeficiency disease (SCID) yielded a small primitive cell population (<4% of thymocytes) that expressed CD117 and CD44 (Pgp-1), which are characteristic of hematopoietic progenitors (Fig. 1B) (*3*). Preliminary results showed that either the combination of phorbol myristate acetate (PMA) and ionomycin or cocultivation with certain stroma cell lines could support progression from the $CD25^-$ to the $CD25^+$ stage after 18 to 24 hours of incubation in vitro (*8*). These experiments also showed that the ability of stromal lines to stimulate CD25 expression directly correlated with their ability to produce TNF-α (*8*). We found that the direct addition of TNF-α (50 ng/ml), a cytokine produced by thymic stromal cells, to $CD117^+CD25^-$ thymocytes induced CD25 expression in a 24-hour assay (Fig. 2A). Induction of CD25 expression was also observed with IL-1α (50 ng/ml) (Fig. 2A), another cytokine produced by thymic stromal cells that shares many biological properties with TNF-α (*9*), but not with 100 ng/ml of other cytokines such as lymphotoxin or IL-6 (Fig. 2A). Treatment with TNF-α and IL-1α together gave an additive effect, which suggested that either cytokine alone was sufficient to promote CD25 expression. The addition of IL-7 resulted in increased recovery of viable $CD25^+$ thymocytes in 24-hour cultures with TNF-α, IL-1α, or both (Fig. 2A) (*10, 11*). SCF was also added in all experiments to enhance thymocyte viability (*3*). Other markers, CD59 (*12*) and high expression of Thy-1, which are characteristic of the $CD25^+$ stage in vivo, were also induced by TNF-α and IL-1α (*13*), and CD25 induction occurred exclusively on $CD117^+$ thymocytes (Fig. 2B). Thus, treatment of the $CD25^-$ progenitors with TNF-α and IL-1α caused them to reach a $CD25^+$ phenotype in vitro similar to that of $CD25^+$ thymocytes in vivo.

We next performed a thymic reconstitution assay to investigate whether the $CD117^+CD25^+$ stage was a necessary step in thymocyte development and to assess directly the role of TNF-α and IL-1α in early thymocyte differentiation (*14*). Hematopoietic cells of fetal thymuses were depleted with deoxyguanosine to create thymic stromal "shells." Then, fetal liver stem cells were added to recapitulate the first stages of thymic development (Fig. 3A). After a 5-day culture, addition of control antibodies to the deoxyguanosine–fetal thymic organ cultures (dGuoFTOC) reconstituted with the fetal liver cells did not prevent the emergence of a large fraction of lymphocytes (18.9%) expressing CD25. However, when neutralizing antibodies to both IL-1α and TNF-α were added, few $CD25^+$ thymocytes (1.7%) appeared (Fig. 3A). Addition of either anti–IL-1α or anti–TNF-α alone did not block CD25 expression (*8*), which confirmed that IL-1α and TNF-α perform overlapping or compensatory functions in the generation of $CD25^+$ thymocytes. All hematopoietic cells detected were of donor origin (Fig. 3A), and no lymphocytes were recovered without the addition of fetal liver stem cells (*8, 14*). We also noted a 21% reduction in Thy-1^{hi} cells and an increase of Thy-1^{lo} cells in treated cultures as compared to control cultures; this finding provided independent evidence that the $CD25^+$ stage, which is accompanied by high Thy-1 expression, was not reached (Fig. 3A). Thus, these cytokines participate in the normal stromal signals that mediate advancement to the $CD25^+$ stage of thymic differentiation.

To determine the effect of preventing the $CD25^+$ stage on overall thymocyte development, we performed longer reconstitution assays. A 9-day culture of control dGuo-FTOC led to the emergence of a large number of double-positive $CD4^+CD8^+$ thymocytes (51.6%) as well as single-positive $CD4^+$ and $CD8^+$ thymocytes (1.4 and 8.9%, respectively). In antibody-blocked dGuo-FTOC, fewer double-positive cells (0.8%) and single-positive $CD4^+$ cells (0.1%) or $CD8^+$ cells (0.4%) emerged (Fig. 3B). Reconstituted dGuoFTOC treated for 5 days with neutralizing antibodies and cultured for six more

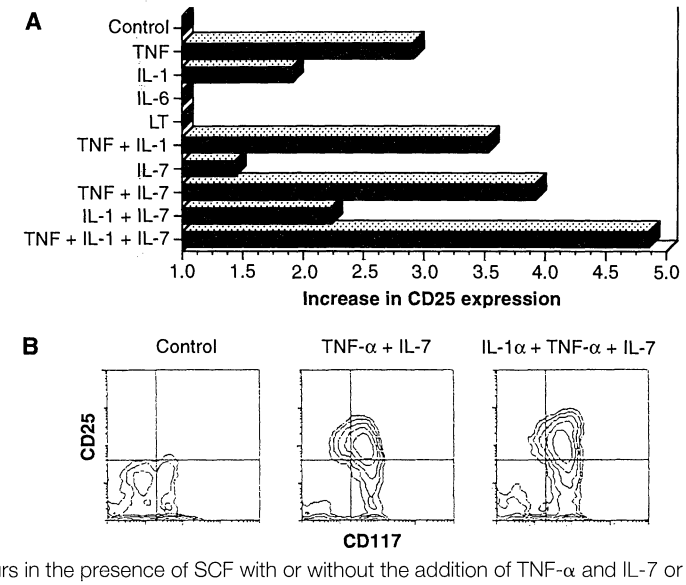

Fig. 2. In vitro induction of CD25 expression on HSA^-CD25^- day 15 fetal thymocytes by treatment with TNF-α, IL-1α, and IL-7. (**A**) Increases in CD25 expression (multiples of baseline amount) as determined by flow cytometry after a 24-hour incubation in SCF with additional cytokines as indicated (*17*). No lymphokine was added in the control condition; no increase in CD25 expression over the control was observed with IL-6 or LT. (**B**) Two-color flow cytometry analysis of CD25 and CD117 expression from isolated immature $CD25^-$ HSA^- SCID thymocytes (Fig. 1C) cultured for 36 hours in the presence of SCF with or without the addition of TNF-α and IL-7 or of IL-1α, TNF-α, and IL-7 (*17*). Percent staining for CD117 versus CD25: Control cultures, UL, 0.8%; UR, 1.8%; LL, 62.4%; and LR, 35.1%. TNF-α + IL-7 cultures, UL, 11.3%; UR, 59.5%; LL, 10.1%; and LR, 19.1%. IL-1α + TNF-α + IL-7 cultures, UL, 4.1%; UR, 56.0%; LL, 14.7%; and LR, 25.2%.

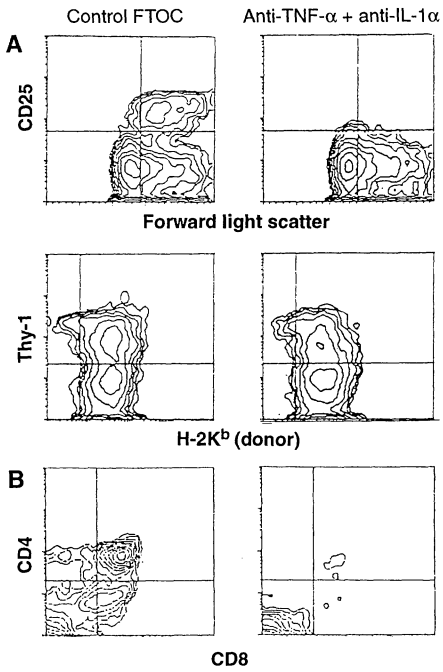

Fig. 3. Neutralization of TNF-α and IL-1α prevents CD25 expression on developing thymocytes and interferes with $CD4^+CD8^+$ thymocyte differentiation. Fetal liver (C57BL/6)–reconstituted dGuoFTOC (BALB/c) were treated with neutralizing antibodies to TNF-α and IL-1α, and control cultures were given irrelevant antibodies (*18*). (**A**) Two-color flow cytometry analysis of day 5 reconstituted dGuoFTOC. Percent staining for forward light scatter versus CD25: Control FTOC, UL, 2.9%; UR, 18.9%; LL, 38.9%; and LR, 40.1%. Anti–TNF-α + anti–IL-1α FTOC, UL, 1.1%; UR, 1.7%; LL, 51.8%; and LR, 45.4%. Percent staining for H-2K^b (donor) versus Thy-1: Control FTOC, UL, 2.0%; UR, 49.0%; LL, 0.8%; and LR, 48.4%. Anti–TNF-α + anti–IL-1α FTOC, UL, 2.5%; UR, 38.8%; LL, 0.8%; and LR, 57.9%. (**B**) Two-color flow cytometry analysis of day 9 dGuoFTOC. Percent staining for CD8 versus CD4: Control FTOC, UL, 1.4%; UR, 51.6%; LL, 38.1%; and LR, 8.9%. Anti–TNF-α + anti–IL-1α FTOC, UL, 0.1%; UR, 0.8%; LL, 96.7%; and LR, 0.4%.

days after removal of the antibodies showed a restoration of development to the double- and single-positive stages (*8*). Thus, stromal cytokine signals that lead to the $CD25^+$ stage are obligatory for further maturation and attainment of the double-positive stage.

After acquiring CD25 and losing CD117 expression, thymocytes initiate TCR rearrangement (*3*). This observation suggested that attainment of the $CD25^+$ stage may be intimately linked to T cell lineage commitment. We isolated $CD117^+CD25^-$ and $CD117^+CD25^+$ day 14 to 15 fetal thymocytes from C57BL/6 (Ly5.1) mice by fluorescent cell sorting and intravenously injected these populations or day 13 fetal liver cells into sublethally irradiated congenic mice (Ly5.2). Because $CD117^+CD25^-$ and $CD117^+CD25^+$ thymocytes share the ability to give rise to T cells after intrathymic transfer (*8*), their function as T cell precursors was not at issue; however, their ability to give rise to other lineages has not been compared (*2*, *3*). Thymocyte progenitors are known to repopulate lymphoid lineages but not myeloid lineages (*2*) and thus may contain committed lymphoid progenitors. We therefore tested for donor reconstitution of B lymphocytes and natural killer (NK) cells. Both fetal liver cells and $CD117^+CD25^-$ thymocytes gave rise to B lymphocytes and to NK cells of donor origin (Ly5.1) in irradiated host mice (Fig. 4). Therefore, the $CD117^+CD25^-$ fetal precursor population can generate multiple lymphoid lineages and may be functionally analogous to $CD4^{lo}CD117^+$ thymocytes in the adult thymus (*2*). In contrast, B cells and NK cells of donor origin were not detected after injection of the same number of $CD117^+CD25^+$ thymocytes (Fig. 4). Neither $CD117^+CD25^-$ nor $CD117^+CD25^+$ progenitors gave reconstitution of T cells in the thymus or peripheral lymphoid compartments, which suggested that fetal thymic progenitors may lose their capacity to home back to the thymus (*8*). Thus, commitment to the T cell lineage and loss of multipotency occur at the stage when $CD117^+$ progenitors express CD25.

Our study has sought to dissect the molecules involved in controlling one of the first stages of thymocyte development. We have shown that critical stromal signals for thymocyte development are mediated by TNF-α and IL-1α. The simplest interpretation of our data is that TNF-α and IL-1α act directly on lymphocyte precursors, but it is also possible that these cytokines act indirectly on a non–T cell subset that is critical for T cell maturation. The fact that all mouse thymocytes go through a $CD25^+$ stage suggests that TNF-α– and IL-1α–mediated precursor differentiation, which includes CD25 expression, represents a necessary step during T cell development and that further maturation to double-positive thymocytes is severely impaired by prevention of the $CD25^+$ stage. Our results do not indicate any direct role for CD25 in thymocyte differentiation. Although attainment of the $CD25^+$ stage by $CD117^+$ thymocytes is permissive for further T cell differentiation, it is also restrictive in that precursor activity for B or NK lymphocytes is lost. The identification of TNF-α and IL-1α as critical influences on these processes will allow further investigation into the molecular mechanism by which differentiation and lineage commitment are achieved through interactions between developing thymocytes and stromal cells.

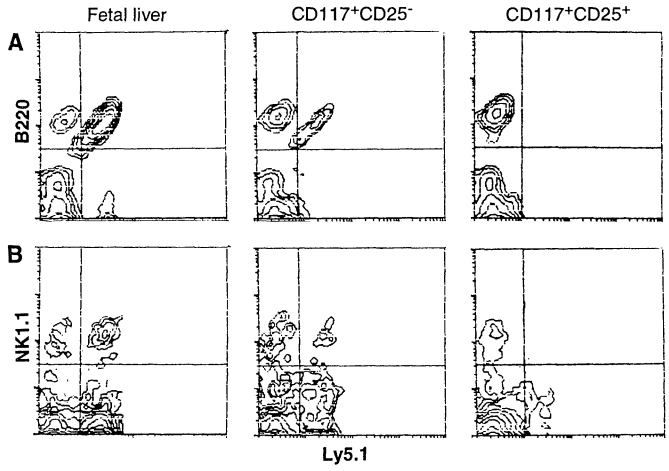

Fig. 4. $CD117^+CD25^-$ but not $CD117^+CD25^+$ fetal thymocytes contain multipotent progenitors for B and NK cells. $CD117^+$ day 15 fetal thymocytes with or without CD25 expression were sorted by flow cytometry and intravenously injected into irradiated congenic host mice (*19*). Flow cytometry analysis of pooled spleen and lymph node cells was performed 22 days after transfer for donor-derived CD45 expression (Ly5.1) on B cells (**A**) or NK cells (**B**). A greater number of contours are plotted in (B) than in (A) to clearly display the recovery of small numbers of NK cells. Control mice were given day 13 fetal liver cells. Percent staining for Ly5.1 versus B220: Mice reconstituted with fetal liver cells, UL, 5.6%; UR, 54.2%; LL, 35.6%; and LR, 4.6%. Mice reconstituted with $CD117^+CD25^-$, UL, 14.5%; UR, 8.9%; LL, 71.8%; and LR, 4.8%. Mice reconstituted with $CD117^+CD25^+$, UL, 28.5%; UR, 0.2%; LL, 70.0%; and LR, 1.3%. Percent staining for Ly5.1 versus NK1.1: Mice reconstituted with fetal liver cells, UL, 0.7%; UR, 2.6%; LL, 35.3%; and LR, 61.4%. Mice reconstituted with $CD117^+CD25^-$, UL, 1.6%; UR, 0.5%; LL, 82.3%; and LR, 15.6%. Mice reconstituted with $CD117^+CD25^+$, UL, 1.8%; UR, 0.1%; LL, 95.3%; and LR, 2.9%.

REFERENCES AND NOTES

1. B. J. Fowlkes and D. M. Pardoll, *Adv. Immunol.* **44**, 207 (1989); K. Ikuta *et al.*, *Cell* **62**, 863 (1990); G. J. Spangrude, S. Heimfeld, I. L. Weissman, *Science* **241**, 58 (1988); C. T. Jordan, J. P. McKearn, I. R. Lemischka, *Cell* **61**, 953 (1990); S. E. Bell and R. Zamoyska, *Eur. J. Immunol.* **21**, 2931 (1991); E. V. Rothenberg, *Adv. Immunol.* **51**, 85 (1992).
2. R. Scollay *et al.*, *Immunol. Rev.* **104**, 81 (1988); L. A. Husmann, R. P. Shimonkevitz, I. N. Crispe, M. J. Bevan, *J. Immunol.* **141**, 736 (1988); J. Nikolic-Zugic, *Immunol. Today* **12**, 65 (1991); R. Scollay, *Curr. Opin. Immunol.* **3**, 204 (1991); L. Wu *et al.*, *Nature* **349**, 71 (1991); L. Wu, M. Antica, G. R. Johnson, R. Scollay, K. Shortman, *J. Exp. Med.* **174**, 1617 (1991); M. Antica, L. Wu, K. Shortman, R. Scollay, *J. Immunol.* **151**, 5887 (1993).
3. M. Ogawa *et al.*, *J. Exp. Med.* **174**, 63 (1991); K. Ikuta and I. Weissman, *Proc. Natl. Acad. Sci. U.S.A.* **89**, 1502 (1992); D. I. Godfrey, A. Zlotnik, T. Suda, *J. Immunol.* **149**, 2281 (1992); D. I. Godfrey and A. Zlotnik, *Immunol. Today* **14**, 547 (1993); D. I. Godfrey, J. Kennedy, P. Mombaerts, S. Tonegawa, A. Zlotnik, *J. Immunol.* **152**, 4783 (1994); T. Moore, S. Huang, L. W. M. M. Terstappen, M. Bennett, V. Kumar, *ibid.* **153**, 4978 (1994).
4. R. Ceredig, J. W. Lowenthal, M. Nabholz, H. R. MacDonald, *Nature* **314**, 98 (1985); D. H. Raulet, *ibid.*, p. 101; R. P. Shimonkevitz, L. A. Husmann, M. J. Bevan, I. N. Crispe, *ibid.* **329**, 157 (1987); D. I. Godfrey, J. Kennedy, T. Suda, A. Zlotnik, *J. Immunol.* **150**, 4244 (1993).
5. H. Schorle, T. Holtschke, T. Hünig, A. Schimpl, I. Horak, *Nature* **352**, 621 (1991).
6. V. Ivanov and R. Ceredig, *Int. Immunol.* **4**, 729 (1992); D. Chen and E. V. Rothenberg, *Mol. Cell. Biol.* **13**, 228 (1993); J. C. Zúñiga-Pflücker, H. L. Schwartz, M. J. Lenardo, *J. Exp. Med.* **178**, 1139 (1993); J. Sen, Y. Shinkai, F. W. Alt, R. Sen, S. J. Burakoff, *ibid.* **180**, 2321 (1994).
7. K. A. Smith, *Science* **240**, 1169 (1988); G. R. Crabtree, *ibid.* **243**, 355 (1989).
8. J. C. Zúñiga-Pflücker and M. J. Lenardo, unpublished observations.
9. C. Dinarello, *Adv. Immunol.* **44**, 153 (1989); B. Beutler and A. Cerami, *Annu. Rev. Immunol.* **7**, 625 (1989); L. Osborn, S. Kunkel, G. J. Nabel, *Proc. Natl. Acad. Sci. U.S.A.* **86**, 2336 (1989).
10. C. S. Henny, *Immunol. Today* **10**, 170 (1989); J. D. Watson, P. J. Morrisey, A. E. Namen, P. J. Conlon, M. B. Widmer, *J. Immunol.* **143**, 1215 (1989); S. R. Carding, A. C. Hayday, K. Bottomly, *Immunol. Today* **12**, 239 (1991); T. Suda, R. Murray, C. Guidos, A. Zlotnik, *J. Immunol.* **144**, 3039 (1990).
11. R. A. Montgomery and M. J. Dallman, *J. Immunol.* **147**, 554 (1991); B. P. Giroir, T. Brown, B. Beutler, *Proc. Natl. Acad. Sci. U.S.A.* **89**, 4864 (1992); N. C. Moore, G. Anderson, C. A. Smith, J. J. T. Owen, E. J. Jenkinson, *Eur. J. Immunol.* **23**, 922 (1993); E. V. Rothenberg and R. A. Diamond, *ibid.* **24**, 24 (1994).
12. K. L. Rock, H. Reiser, A. Bamazai, J. McGew, B. Benacerraf, *Immunol. Rev.* **111**, 195 (1989).
13. HSA^-CD25^- thymocytes (1×10^5 to 3×10^5) (Fig. 1) were cultured for 24 hours in a round-bottom 96-well microtiter plate in 200 μl of Click's medium (Biofluids, Rockville, MD) with 10% fetal calf serum (Fig. 2). After staining with D7 monoclonal antibody (Pharmingen, San Diego, CA) (*12*), flow cytometry analysis revealed that treatment with TNF-α, IL-1α, IL-7, and SCF induced expression of CD59 (Ly6A/E) that was 4.35 times the amount of CD59 expression on control cultures that only received SCF (8 to 11%). These data correspond to the average of duplicate cultures.
14. E. J. Jenkinson, L. Franchi, R. Kingston, J. J. T. Owen, *Eur. J. Immunol.* **12**, 583 (1982); R. Kingston, E. J. Jenkinson, J. J. T. Owen, *Nature* **317**, 811 (1985).
15. Fetal liver or thymus single-cell suspensions from timed pregnant C57BL/6 mice (National Cancer Institute, Frederick Cancer Research and Development Center, Frederick, MD) were incubated with monoclonal antibodies

specific for CD25 and CD117 (Pharmingen) and were analyzed with a FACScan (Becton Dickinson, Mountain View, CA) flow cytometer and Lysis II software. The specificity of antibody staining was confirmed with isotype-matched control antibodies. CD117 expression was similar to that previously reported (*3*).

16. HSA$^-$CD25$^-$ day 14 to 15 fetal and neonatal SCID thymocytes were obtained by antibody- and complement-mediated lysis. Single-cell suspensions of thymocytes (25×10^6 to 30×10^6 cells) were incubated on ice with 300 μl of culture supernatant of J11d.2 (anti-HSA) and 7D4 (anti-CD25) for 15 min, Low-Tox rabbit complement (Cedar Lane, Hornby, Ontario) was added, and cells were incubated at 37°C for 30 min. After complement-mediated lysis, viable cells were recovered by density centrifugation with Lympholyte-M (Cedar Lane). CD25$^-$HSA$^-$ thymocytes represented 4% of total day 15 fetal or neonatal SCID thymocytes. CD25$^+$HSA$^+$ thymocytes represented freshly isolated cells that were not treated with anti-CD25 or anti-HSA.
17. HSA$^-$CD25$^-$ day 14 to 15 fetal and neonatal SCID thymocytes (1×10^5 to 3×10^5) (*16*) were cultured for 24 hours in round-bottom 96-well microtiter plates in 200 μl of Click's medium (Biofluids) with 10% fetal calf serum. All cytokines were obtained from R&D Systems (Minneapolis, MN). TNF-α, IL-1α, and IL-7 were used at 50 ng/ml, IL-6 and lymphotoxin (LT) were used at 100 ng/ml, and SCF was used at 20 ng/ml. Cell recovery was not affected by the addition of TNF-α or IL-1α; however, addition of IL-7 increased total cell recovery by 30 to 40% in both the control and treated cultures. CD25 expression on control (SCF only) cultures was 5 to 10%. The increase of CD25 expression compared to its expression in control cultures was determined by flow cytometry. CD25 induction was not a result of outgrowth of a CD25$^+$ subpopulation because (i) cell yields in cultures with or without TNF-α treatment were similar, (ii) no cellular turnover was observed, and (iii) CD25 expression could be detected as early as 8 hours after treatment (Fig. 2A) (*8*). In Fig. 2B, SCID thymocytes gave better cell yield in culture, resulting in greater recovery of CD25$^+$ cells. The data shown correspond to the average of triplicate cultures and are representative of at least five independent trials.
18. Day 15 fetal thymuses (BALB/c) were placed in organ culture for 6 days in the presence of 1.0 mM deoxyguanosine (*14*) and then washed for 1 day before reconstitution. Day 13 fetal liver cells (C57BL/6) (3×10^4) were used to reconstitute the thymic shells in a hanging drop setup for 24 hours (*14*). Reconstituted dGuoFTOC were then cultured, under standard FTOC conditions (*14*), for 5 or 9 days before flow cytometry analysis. Antibodies to mouse TNF-α, mouse IL-1α, and human interferon γ (control) were obtained from Genzyme (Cambridge, MA). Antibodies were used at a final dilution in stock of 1:80. Antibodies were added every other day, starting with day 1, to the FTOC. No changes in cell recovery were observed by day 5 of culture; however, by day 9, 30% fewer cells were usually recovered per thymic lobe from the antibody-treated FTOC.
19. Day 14 to 15 fetal thymocytes, which had been gated for lack of CD3 expression to exclude mature γδ T cells, were sorted by flow cytometry into CD117$^+$ thymocytes with or without coexpression of CD25. Day 13 fetal liver cells (1×10^5) or sorted day 14 to 15 fetal thymocytes (2×10^5 to 3×10^5) (>98% purity; FACStar-plus, Becton Dickinson) were intravenously injected into Ly5 congenic host mice irradiated with 7.5 Gy (750 rads). After 22 days, peripheral lymphocytes (pooled spleen and lymph nodes) were collected and analyzed for donor-derived lymphocytes.
20. We thank C. Eigst and D. Stephany for fluorescent cell sorting and R. N. Germain, B. J. Fowlkes, P. Schwartzberg, and M. H. Julius for reading the manuscript. Supported by the Jane Coffin Childs Memorial Fund for Medical Research (J.C.Z.-P.) and Cancer Research Institute (M.J.L.).

6 February 1995; accepted 24 April 1995

Isolation of an hMSH2-p160 Heterodimer That Restores DNA Mismatch Repair to Tumor Cells

James T. Drummond,* Guo-Min Li,* Matthew J. Longley, Paul Modrich†

A mismatch-binding heterodimer of hMSH2 and a 160-kilodalton polypeptide has been isolated from HeLa cells by virtue of its ability to restore mismatch repair to nuclear extracts of hMSH2-deficient LoVo colorectal tumor cells. This heterodimer, designated hMutSα, also restores mismatch repair to extracts of alkylation-tolerant MT1 lymphoblastoid cells and HCT-15 colorectal tumor cells, which are selectively defective in the repair of base-base and single-nucleotide insertion-deletion mismatches. Because HCT-15 cells appear to be free of hMSH2 mutations, this selective repair defect is likely a result of a deficiency of the hMutSα 160-kilodalton subunit, and mutations in the corresponding gene may confer hypermutability and cancer predisposition.

Certain sporadic cancers and virtually all tumors that occur in patients with hereditary nonpolyposis colorectal cancer (HNPCC) are characterized by a high incidence of mutation in microsatellite repeat sequences [reviewed in (*1*)], and cell lines derived from such tumors are genetically unstable (*2–4*). Cancer predisposition in most HNPCC kindreds is attributable to defects in any one of four genes, all of which encode homologs of the microbial mismatch repair proteins MutS and MutL. The *hMSH2* gene specifies a MutS homolog (*5*), whereas *hMLH1*, *hPMS1*, and *hPMS2* encode homologs of MutL (*6*, *7*).

J. T. Drummond and P. Modrich, Howard Hughes Medical Institute and Department of Biochemistry, Duke University Medical Center, Durham, NC 27710, USA.
G.-M. Li and M. J. Longley, Department of Biochemistry, Duke University Medical Center, Durham, NC 27710, USA.

*These authors contributed equally to this work.
†To whom correspondence should be addressed.

As judged by biochemical assay, tumor cells that display microsatellite instability are typically defective in mismatch correction (*2*, *8*), thus providing a direct link between the HNPCC genes and genetic stability afforded by this DNA repair system. For example, the H6 and LoVo colorectal tumor cell lines, which are defective in both alleles of *hMLH1* and *hMSH2*, respectively (*6*, *8*), are both defective in mismatch repair. An activity that restores mismatch repair to extracts of *hMLH1*-deficient H6 cells has been isolated from HeLa cells and shown to be a heterodimer of hMLH1 and hPMS2 (*9*).

Although hMSH2 has been shown to bind mismatched base pairs (*10*, *11*), the form of the protein active in mismatch repair has not been defined. To clarify this issue, we isolated from HeLa cells a component that restores mismatch repair to nuclear extracts of LoVo cells (*12*). This complementing activity, designated hMutSα, is associated with two polypeptides of 105 kD and 160 kD (Fig. 1A). The 105-kD protein was shown by immunoblot to be hMSH2 (Fig. 1B). The molar equivalence of the two polypeptides (*13*) suggested that they might interact. To test this possibility, we monitored the protein composition and activity of purified hMutSα (*12*) during gel permeation chromatography and band sedimentation through sucrose density gradients (*14*). Association of the two polypeptides and their relative stoichiometry (0.92 ± 0.05 mol per 1 mol, $n = 5$) were preserved during these procedures.

We estimated the native relative molecular mass of hMutSα on the basis of its Stokes' radius (R_S; 67 Å), its sedimentation coefficient (9.0S), and the partial specific volume of the subunits (*14*, *15*). Assuming a typical protein partial specific volume of 0.725 cm^3/g for p160 (*15*) and a calculated partial specific volume (*16*) of 0.741 cm^3/g for hMSH2 based on the predicted amino acid sequence (*5*), these hydrodynamic parameters indicate a native molecular mass of 255 kD. Because this value is close to that expected for a 1:1 complex of the two polypeptides, we conclude that hMSH2 functions in mismatch repair as one subunit of a heterodimer, the other component of which is p160.

To identify p160, we sequenced five internal tryptic peptides derived from the protein (*17*). None of the peptides showed significant homology to proteins in the National Center for Biotechnology Information (NCBI) nonredundant sequence database. This finding, and the highly specific response of hMSH2 antibodies to the 105-kD polypeptide of hMutSα, demonstrate that p160 and hMSH2 subunits are distinct at the sequence level and are thus